

	LOW pH CONDITIONS	High pH CONDITIONS
LiOH (ppm Li)	0.2	2.2
H <sub>3</sub> BO <sub>3</sub> (ppm B)	650	500
H <sub>2</sub> (cm <sup>3</sup> /kg SPT)	25 - 50	25 - 50
O <sub>2</sub> (ppb)	< 5	< 5

TABLE 4  
-----

CHEMISTRY CONDITIONS OF TWO CIRENE TESTS

## OBSERVATIONS OF CRUD DEPOSITS, CORROSION AND EROSION OF BWR AND PWR FUEL

H. BAIRIOT  
Belgonucléaire,  
Brussels

P. DE REGGE  
SCK/CEN  
Mol

Belgium

### Abstract

The BWR experience is limited to one reactor but the PWR experience covers a wide range of successive generations of power plants (7 in total). The systems are described and their water chemistry briefly commented. Some R&D performed on the effects of the operating regimes (steady state and transients) are summarized.

Observations made by post-irradiation examinations and postirradiation examinations of fuel are outlined concerning water chemistry effects (crud deposits and corrosion) and "mechanical" coolant-cladding interaction (chip deposits and baffle jetting).

### 1. INTRODUCTION

Nuclear power started to be produced in Belgium in 1962 when the BR 3 plant was connected to the grid. This plant and all the successive ones are PWR's and represent the complete evolution from the rather modest power densities typical of the sixties up to the ones representative of modern designs (Table I)

56 The initial operating conditions of BR 3 were very conservative but have been updated. At the present time, this power plant is partially devoted to development and testing of nuclear fuel. The core design takes into account that some experimental fuel rods require representative fuel irradiation conditions (LINGR), while others require representative cladding irradiation conditions (average cladding temperature); the latter is obtained by operating those rods at high heat ratings, as illustrated in Table 1. It has enabled to obtain representative data for what concerns clad oxidation and crud deposition. The initial cores consisted of stainless steel cladding; Zircaloy 4 was progressively replacing stainless steel from 1969 on. It afforded the possibility of comparing the behaviour of those two cladding materials irradiated simultaneously. The CNA plant was also updated by a factor 1.34 from its initial design power, partially by reducing the number of assemblies in the core and partially by increasing the reactor power. It is still operated with stainless steel clad fuel rods.

The Dodewaard power plant is operated by GKN (the Netherlands). Comparative characteristics of this rather early design of BWR's and modern ones are given in Table 2. Dodewaard has mainly been utilized, in the frame of the Belgian R&D programme on nuclear fuels, to investigate multiple fuel design aspects and, in particular, to compare various surface treatments of the fuel claddings and alternative spacer grid designs; it provides indeed representative environment conditions for testing BWR fuel.

The present paper will outline a few observations collected from those power plants.

## 2. WATER CHEMISTRY OF THE PWR'S

The particular case of DOEL 1 & 2 will be used as an example, since it has been studied in detail [1].

### 2.1. Description of DOEL 1 and 2

The reactor vessel is 10.60 m high with an internal diameter of 3.33 m; it is made of carbon steel coated inside with stainless steel.

The reactor core consists of 121 fuel assemblies, each of them containing 179 fuel rods and 17 guide-thimbles for the control rod cluster, instrumentation, neutron sources and burnable poison. The fuel assembly has a square section of  $0.197 \times 0.197 \text{ m}^2$  and a total length of 2.853 m. The Zircaloy-4 cladding has an external diameter of 10.7 mm. The total surface of Zircaloy-4 amounts to  $\approx 2270 \text{ m}^2$ .

The 33 control rod clusters consist of an Ag-In-Cd-alloy in a stainless steel cladding; the control rods glide in guide-thimbles which are part of the fuel assembly structure.

The two steam generators each contain 3260 U-tubes; the total surface for heat transport to the secondary system equals  $4130 \text{ m}^2$ . Tubes are Inconel 600 and the water chambers under the pipeplate are coated with stainless steel. The different components of the primary coolant are connected with stainless steel tubes.

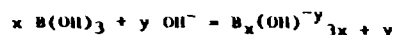
The circulation pumps are placed on the cold legs: wear surfaces are made of stellite, which is essentially a cobalt-chromium-tungsten carbon alloy. Stellites have been developed for their resistance to wear, to oxidation and corrosion at elevated temperatures and to a wide range of chemicals. Because of their use in the pumps, stellites are however subject to some mechanical wear and erosion. The processes can cause the release of significant amounts of cobalt, chromium and tungsten into the primary circuit and eventually the build-up of longlived activation products [2, 3].

### 2.2. Adopted chemistry

The cooling water of the PWR's DOEL 1 ("KCD1") and DOEL 2 ("KCD2") is pressurized at 15.4 MPa ( $157 \text{ kg/cm}^2$ ) and has an average core temperature of  $286^\circ\text{C}$  (zero power) to  $302^\circ\text{C}$  (maximum power).

The concentration of boric acid as a function of burnup is illustrated in figure 2.1, during the reactor cycle. During shutdown and refuelling, the boric concentration is increased to 1900 ppm B.

Boric acid added to the water forms different ionic species defined by the general equation :



The significant species formed at high temperature and moderate alkalinities are  $\text{B(OH)}_3$ ,  $\text{B(OH)}_4^-$ ,  $\text{B}_2(\text{OH})_7^-$  and  $\text{B}_3(\text{OH})_{10}^-$  [4]. The dependence of the equilibrium constant on temperature and ionic strength is discussed in [1].

At high temperatures boric acid is a weak acid, indicated by the decreasing difference in pH between the solution with 1500 ppm B (as boric acid) and pure water. The same solution with  $10^{-4}$  molal strong base (e.g. KOH) is significantly alkaline with respect to pure water at 300° C.

As a rule, the corrosion of iron and nickel based alloys is lowest in moderately alkaline solutions. Therefore  $^7\text{LiOH}$  is added to the coolant.  $^7\text{Li}$  has a low neutron capture cross-section and does not form radioactive products. Additional  $^7\text{Li}$  is produced by the reaction  $^{10}\text{B} (n, \alpha) ^7\text{Li}$ . Naturally occurring lithium contains only 7%  $^7\text{Li}$  and 93%  $^6\text{Li}$ . The latter isotope undergoes the reaction  $^6\text{Li} (n, \alpha) ^3\text{H}$ , to form undesirable tritium. Therefore naturally occurring lithium is enriched to 99.9%  $^7\text{Li}$ .  $\text{LiOH}$  is a slightly weaker base than  $\text{NaOH}$  or  $\text{KOH}$  at high temperatures. For the DOEL 1 and DOEL 2 power plant, boric acid concentration varies from zero to 1200 ppm B, and the  $\text{LiOH}$ -concentration from  $\approx 400 \mu\text{g l}^{-1}$  to  $\approx 2000 \mu\text{g l}^{-1}$ , in a way that an almost constant pH of 6.5 is maintained.

The radiolysis of water in nuclear power reactors has been investigated exhaustively by many scientists and several books describe the general principles [5]. Simplistically, ionizing radiation decomposes water to form  $\text{H}^+$ ,  $\text{OH}^-$ ,  $\text{H}$ ,  $\text{OH}$ ,  $\text{H}_2$ ,  $\text{O}_2$ ,  $\text{H}_2\text{O}_2$ ,  $e_{\text{aq}}^-$  and  $\text{HO}_2^-$ . The stable products are  $\text{H}_2$ ,  $\text{O}_2$  and  $\text{H}_2\text{O}_2$ . The other species are intermediates (which decay) or ionic forms but their ephemeral presence near the cladding surface may be a cause of the observed irradiation induced corrosion enhancement. The  $\text{O}_2$  and  $\text{H}_2\text{O}_2$ , formed continuously in the water, accelerates corrosion of the

structural materials. To cope with this problem,  $\text{H}_2$  is added to water in such an amount as to achieve undetectable levels of  $\text{O}_2$  and  $\text{H}_2\text{O}_2$ . For the power plants DOEL 1 and DOEL 2, the  $\text{H}_2$ -concentration in the primary coolant is maintained at  $36 \pm 5 \text{ cm}^3\text{H}_2/\text{kg}$ .

### 2.3. Characterization of corrosion particles

#### 2.3.1. During steady state regime of the reactor.

Coolant data during one reactor cycle are summarized in Table 3. The primary coolant contains a lot of corrosion products, which are present at a concentration of a few ppb. The major part of these elements are present in the form of crud particles in suspension as can be seen in Table 5; the normal range of crud present in the coolant is 50 to 500  $\mu\text{g/l}$ . Table 6 gives typical inventories of fission and activation products resulting from fissions of uranium contaminating the surfaces, leakage through cladding defects and neutron capture reactions. A more detailed analysis of the filterable fraction of the activity reveals  $^{58}\text{Co}$ ,  $^{51}\text{Cr}$ ,  $^{60}\text{Co}$ ,  $^{54}\text{Mn}$  and  $^{59}\text{Fe}$  as the most important isotopes. Table 7 gives the specific activity of the isotopes as Bq per mg crud.

On the basis of those data and similar measurements the following conclusion can be made :

- The activation products are the main source of plant radiation levels during shutdown.  $^{58}\text{Co}$  and  $^{51}\text{Cr}$  each account for 45% of the total radioactivity, and,  $^{60}\text{Co}$ ,  $^{54}\text{Mn}$  and  $^{59}\text{Fe}$  for a few %.
- The activity level of these isotopes is higher for KCD 2 than for KCD 1, although these are twin plants operated within the same specifications.
- The activation products occur in the coolant mainly as particles in suspension, except for  $^{54}\text{Mn}$  which is deduced to be partly (40 to 60%) present in soluble form in the coolant.
- The distribution of the activity over the filter membranes indicates that about 80% of the filterable activity is associated with particles greater than 2  $\mu\text{m}$ . The remaining activity is about equally distributed over the smaller particles.

50 e. The specific activity of the crud is a function of the particle diameter (Table 7). Particles greater than  $2 \mu\text{m}$   $\phi$  have a significantly greater specific activity than the smaller ones. The smallest particles ( $\phi$   $0.1 \mu\text{m}$ ) have a somewhat greater specific activity than the medium size particles.

f. Treatments of the coolant with ion exchange resins (mixed bed) show that  $\sim 2\%$  of the activity in the coolant is captured on the IX. This means that about 6% of the activity that has not been filtered by the filter membrane with pore size of  $0.1 \mu\text{m}$ , is not present as ions in solutions but associated with particles in suspension with a diameter less than  $0.1 \mu\text{m}$ . The total activity associated with particles in suspension can therefore be estimated at  $\sim 98\%$ .

g.  $^{58}\text{Co}$  is associated with particles in suspension  $> 0.1 \mu\text{m}$  for about 70%.

h. Since  $^{54}\text{Mn}$  was suspected to appear as ions in solution, the coolant was passed through a mixed bed ion exchanger. Only 15% of  $^{54}\text{Mn}$  and 4% of  $^{58}\text{Co}$  were retained on the ion exchange bed, which means that  $^{54}\text{Mn}$  as well is mainly associated with particles in suspension but with a smaller particle size (Table 7).

Since the activity in the primary coolant is mainly associated with particles in suspension, these particles were studied more in detail. A great variety of particles can be observed with or without regular forms, present in clusters or isolated. Stereoscopic examination shows the greater particles as being agglomerates of smaller ones. It is not known if these clusters are present in the coolant or formed during filtration. Therefore it is very difficult to establish a particle size distribution from these SEM pictures.

Chemical analysis by means of the emitted X-rays reveals the presence of Fe, Cr, Ni and Si. By means of point-analysis, it appears that individual particles have a different composition. Fe, Cr and Ni are nearly always detected in changing proportions. Si is detected frequently and elements as Mo, Mn, V, Zr, Tl are usually only present as minor elements.

The Quantimet results give supplementary information about the particle size distribution of the corrosion particles. Figure 2 gives a representation of the particle size distribution. The zone beneath  $0.5 \mu\text{m}$  cannot be explored with the optical microscope.

The corrosion products in the primary coolant have a magnetite or a spinel-type ferrite structure, as determined by X-ray diffraction analysis (Table 8). Magnetite is the double oxide  $\text{FeO}\cdot\text{Fe}_2\text{O}_3$ . In this spinel-type structure Fe II and Fe III can be replaced by other bivalent or trivalent metals of similar atomic radius e.g. Cu, Ni, Cr, Mn, Mg, Zn, Co. The structure  $(\text{Fe},\text{Mg})(\text{Cr},\text{Fe})_2\text{O}_4$  only indicates the presence of a spinel-type structure of undetermined composition, where Fe II and Fe III are replaced by other metals.

#### 2.3.2. During transient phase of the reactor KCD 2

The transient phase under investigation was the normal shutdown procedure to refuelling of the power plant KCD 2 (October 1978). Power-, temperature- and pressure changes are given in figure 3 as a function of time.

For all detectable elements a considerable increase in concentration is observed which begins already during power decrease, reaching a constant level after about 20 hours. The injection of  $\text{H}_2\text{O}_2$  seems to have a limited influence on the release of corrosion products in the coolant. The levels of the concentration in the coolant and the filtrate are comparable indicating the presence of non filterable colloids or ions in solution. Figures 4 and 5 give the variation of the concentration of the elements as a function of time. Results on the particles in suspension are summarized in Table 9. These results confirm that the elements are present in the coolant as very small colloids or ions in solution because the concentration of the elements in the coolant increases considerably without corresponding increase of the suspended particles.

Figures 6 and 7 show the variation of the activity of the primary coolant during the shutdown procedure. At decreasing power the activity increases with a factor 5 to 10 for the four isotopes mentioned. During this phase the activity of the particles in suspension increases as well.

During the first phase of cooling down and boratation the activity in the coolant remains fairly constant. On the other hand the activity associated with particles in suspension decreases, whereby the concentration of the radioisotopes as ions in solution increases by a corresponding amount. During the second phase of the cooling down period a strong boratation to 1900 ppm B takes place and as a consequence the coolant activity increases again with a factor 5 to 10. The activity of particles in suspension remains practically constant and the activity of ions in solution increases parallel with the total activity of the coolant. The addition of  $H_2O_2$  seems to have a limited influence on the activity profile. The  $^{58}Co$  activity changes over a much greater time interval after shutdown. The activity increase takes place during the first day after shutdown and the ions in solution are eliminated by ion exchange treatment over a period of two weeks.

SEM-analyses have been performed to identify the physical structure and chemical composition of the corrosion particles. In addition to the usual forms also present in the coolant under stable conditions, flake-like structures are observed.

X-ray diffraction analysis reveals similar structures as during steady state operations:  $Fe_3O_4$  and the mixed spinel  $(Fe, Mg)(Cr, Fe)_2O_4$ . Samples taken after 40 hours shutdowns apparently lost the structured compounds yielding X-ray diffraction patterns.

In general, during the transient phases of the reactor coolant, the composition of the coolant water is completely disturbed. Due to power decrease, cooling down and boratation the impurity concentration increases strongly from beneath  $50 \mu g l^{-1}$  during steady state to more than  $2000 \mu g l^{-1}$  at 20 hours after shutdown.

The increase of impurity concentration can be subdivided into several steps:

a. During power decrease the activity in the coolant increases by an order of magnitude at nearly constant concentration of suspended particles or total impurities. However the activity is mainly present as suspended material.

b. During the cooling and boratation period both the activity level and the corrosion products concentration increases. During this stage a general dissolution of corrosion products takes place.

During a particular shutdown of the reactor KCD 2, the coolant was passed through a set of membrane filters and a cation- and anion-exchange resin to find out which part of the activity is associated with particles and which part present as ions in solution. Figure 8 summarises the results obtained. As can be seen again about 80% of the  $^{58}Co$  activity is associated with particulates before shutdown. After shutdown the proportion of ions in solution increases to reach about 99% after 6 days. The same pattern occurs for  $^{137}Cs$  which starts however with 85% activity associated with ions in solution. Both ions are present under cationic form for the nuclides indicated with the exception of a few % anionic forms. The general conclusion out from these data is that a few days after shutdown the whole activity is present in the coolant as ions in solution.

#### 2.3.3. During transient phase of the reactor KCD 1

The transient phase investigated was the normal shutdown procedure prior to refuelling of the power plant KCD 1 (March 1979). The general observations were similar to the KCD 2.

#### 2.3.4. CNA observations

The behaviour of corrosion products during the shutdown procedure of KCD 1 and 2 can be compared with similar results obtained at other power plants. During the shutdown of CNA (Chooz) in 1972, about the same procedure has been followed with the exception of a lower boron concentration, 1000 ppm instead of 1900 ppm B for KCD. About the same conclusions can be drawn. However the level of the activity associated with the particles in suspension seems to be much higher for CNA than for KCD. The smaller boratation might be responsible for this.

## 2.4. Lessons learned

### 2.4.1. Nature of the corrosion products

Little work has been reported on the exact nature of the products resulting from corrosion in nuclear reactors. The information that does exist shows that deposits from reactor coolant circuits contain metals, metal oxides and spinel mixed oxides. MacDonald and Rumery [6,7] performed a thermodynamic study of metals and metal oxides in aqueous systems at elevated temperatures; they state that the chemical properties of reactor crud can depend upon the partial pressure of hydrogen and oxygen in the system. Figure 9 presents the equilibrium concentrations of hydrogen in solution for the Ni/NiO and Co/CoO systems. At hydrogen concentrations greater than the equilibrium values the metals are stable. At temperatures less than 150°C only very small concentrations of hydrogen are required to reduce the oxides to their respective metals. At higher temperature, however, the concentration of hydrogen required increases rapidly. In the case of the iron/iron-oxide system, magnetite ( $\text{Fe}_3\text{O}_4$ ) is the stable oxide at these levels of hydrogen over the entire temperature zone of interest.

Many authors report that spinel mixed oxides of the type  $\text{MFe}_2\text{O}_4$  can be formed under the conditions of interest. In view of the possible implication of oxides of this type in radioactivity transport and corrosion phenomena of metals in high temperature aqueous systems, Rumery and MacDonald [7] have examined the thermodynamic stabilities of the ferrites at the levels of oxygen and hydrogen and at the temperatures commonly used in the operation of water cooled nuclear reactors and whether, once formed, the ferrite can be expected to remain in the system without undergoing either oxidation or reduction. For the coolant conditions of KCD 1 + 2 (temperatures of 280° to 300°C, 35 ml/kg of hydrogen and 2.2  $\mu\text{g}/\text{l}$  of oxygen) one would expect to find  $\text{NiFe}_2\text{O}_4$  and  $\text{CoFe}_2\text{O}_4$ . These conditions are so far consistent with the observations made on corrosion products, that mixed spinel structures are found but it was not possible to identify the exact nature of these ferrites. Cobalt is present in the coolant system structural materials in too low quantities to form detectable levels of  $\text{CoFe}_2\text{O}_4$ . In any event, since cobalt is thermodynamically similar to nickel, and since

$\text{NiFe}_2\text{O}_4$  and  $\text{CoFe}_2\text{O}_4$  can form solid solutions, it is likely that cobalt is associated with nickel in  $\text{NiFe}_2\text{O}_4$ . The resultant mixed oxide of the form  $\text{Co}_x\text{Ni}_{1-x}\text{Fe}_2\text{O}_4$  probably behaves similarly to  $\text{NiFe}_2\text{O}_4$  since  $x \ll 1$

### 2.4.2. Transient reactor operations

With the data from KCD 2, confirmed by the results for KCD 1, a general model of the behaviour of corrosion products during shutdown can be drawn. The primary coolant circuit consists of a closed system filled with water. On the walls a layer of oxide material is deposited and in the water phase itself a small amount of corrosion material is circulating as particles in suspension. During transient phases of the reactor, e.g. shutdown procedures, this oxide material dissolves. This generally happens at the wall of the circuit whereby fixed material dissolves directly. Spalling of this oxide layer results in the formation of particulate matter but this process is of limited importance compared to the direct dissolution process. Particles in suspension dissolve as well and slowly decrease in diameter. Several classes of particles are thus formed during dissolution, the greater particle size feeding the smaller ones and simultaneously feeding ions into the solution. By spalling of the oxide layer all fractions are simultaneously fed but this feed term is of minor importance compared to the direct dissolution. The dissolution of deposited oxide layers on the wall is not complete, ending with a partially cleaned surface, with a small amount of particles in suspension and with a considerable amount of dissolved matter. These dissolved elements are separated from the coolant by ion exchange in the purification system of the primary coolant circuit. The model is schematically depicted in Figure 10. Two parameters are influencing the process: temperature and boron concentration. A decreasing temperature from 300°C to 100°C at 20 ppm B results in a steady state situation or a decreased solubility. At higher boron concentrations this decreasing solubility zone is much smaller and lies between 300°C and 270°C. Increasing the boron concentration, especially at low temperature, results in a high solubility increase. The solubility at 50°C is about two orders of magnitude higher when the boron concentration equals 1000 ppm B instead of 20 ppm B. This means that the pH-parameter has much more impact on the dissolution phenomenon than has the temperature parameter. This has indeed been shown in the

results obtained for KCD 1 + 2. The variations in impurity concentration and activity level follow much closer the boron concentration pattern.

### 3. OBSERVATIONS OF CRUD AND CORROSION ON LWR FUELS

The results reported by various investigators indicate two extremes, on the basis of observations performed on irradiated fuel. Some investigators have found crud deposition on fuel to be minor or even nil; only a corrosion layer is observed, with a variability from plant to plant and even from cycle to cycle that imposes to use an arbitrary (best-fit) enhancement factor in the corrosion equations [8]. Others have observed crud deposits to play an important role in most of their observations; the variability of these crud deposits from plant to plant explain most of the variability of the corrosion observed on the cladding.

We are tenant of the second hypothesis : the crud observed on the fuel rod surfaces after irradiation may not be a correct image of the situation during irradiation and crud is known to affect clad OD temperature and therefore corrosion [9]. The present chapter will summarize some observations in that respect. The concurrent data on hydriding will not be reported here, since it justifies a genuine development.

#### 3.1. BR 3 (PWR)

##### 3.1.1. Stainless Steel Claddings

Early fuel irradiated at modest LMR'S (below 130 W/cm) to a modest burnup (6 GWd/tM) presented only a uniform corrosion layer, with no crud deposits [10]. Later fuel irradiated at 200 W/cm to a burnup of 40 GWd/tM presented shallow pits up to 6  $\mu$ m deep. The thin crud deposit (10  $\mu$ m) was filling those pits [11].

##### 3.1.2. Zircaloy Claddings

Crud deposits have been observed in the highest rated rods with an induced influence on clad corrosion. The enhanced corrosion underneath

thick crud layer led to the failure of six fuel rods in one reactor cycle after 380 days [12], at locations of high local heat flux (170 W/cm<sup>2</sup>).

The general observation is that crud deposits are a complex function of :

- the cleaning operations of primary circuit surfaces during previous shutdown (for maintenance and/or inspection)
- the primary coolant chemistry during the reactor operation
- the local heat transfer characteristics at the cladding surface
- the history evolution of those factors.

More time would need to be devoted to the data base to draw comprehensive conclusions. Some considerations are outlined in [12].

#### 3.2. CNA and KCD 1 and 2 (PWR's)

Mostly visual examination on the fuel from those power plants together with the experiments presented in section 2 confirm the more detailed examination made on BR 3 fuel. It suggests that the cold shutdown image of the cladding surface might not be a true representation of the crud layer under operating conditions. In particular, porous crud may dissolve at varying rates depending on the shutdown history.

#### 3.3. Dodewaard (BWR)

Numerous post-irradiation examinations [e.g. 13,14] have confirmed the presence of a thick porous crud layer on the cladding surface; it results from some of the primary circuit being carbon steel. This crud is quite loose and can easily be brushed away. Although Dodewaard is a natural circulation reactor with low coolant velocities, it is obvious that most of this crud can not adhere to the cladding surface under operating conditions. Quite a large amount of the crud is even lost if the fuel assembly or rod is moved rapidly in the pool.

### 3.4. Lessons learned

Crud deposits are a major cause of corrosion enhancement. The variability of observed crud layer from cycle to cycle is a complex function of coolant chemistry, temperature levels and evolution of both during irradiation. Post-irradiation measurements are deceiving since shutdown conditions are altering the crud conditions.

#### 4. MECHANICAL COOLANT/CLADDING INTERACTION

Most attention is devoted to the chemical aspect of CCI. Two particular occurrences in Belgian power plants have recently focused the attention on some mechanical aspects.

##### 4.1. KCD 2 chips incident

4.1.1. During the KCD 2 annual overhaul in 1982, several operations (e.g. pluggings, sleeving, tube pulling) were carried out on the steam generators ("SG"), in relation with the leakage situation which is typical of most PWR's. One of them consisted in drilling holes in the inner walls of the SG nozzles. In spite of the very tight procedures, the quality control inspectors intervening at hold points and documenting each inspection in a report and a quality assurance supervisor inspecting these reports, one chip-catcher had been forgotten in the hot leg nozzle of a SG. After one week of operation, the plant had to be stopped for SG leakage. The metallic debris of the chip-catcher were discovered and removed, but the small drilling chips it contained were already distributed in the primary circuit. The unit was restarted.

4.1.2. In the weeks after the restart, the activity of the primary water raised, indicating multiple fuel damage. Finally the plant reached the technical specification limit of 1 in the secondary circuit and had to be shut-down. A sipping campaign of the whole core revealed three leakers, all of them fresh fuel assemblies (hence with only a weak sipping signal). Visual inspection of the leakers showed some foreign material caught be-

tween fuel rods in the lower spacer grid spans; additional examinations revealed the chips in nearly every fuel assembly.

Most samples were hard to collect, as the material was like welded in place. The chips were highly radioactive, which indicated that they had been in the core for quite a long time (leading to the erroneous conclusion that these were not the steam generator drilling chips). Chemical and spectrometric analysis showed these chips to be metallic, carbon steel for part of them and stainless steel for the other part.

Since chips were found on the route followed by the manipulated fuel assemblies (i.e. on the top of the core baffle and the bottom of the reactor pool), it was clear that some chips were falling out and therefore fairly loose.

4.1.3. It was quite unanimously recommended that the chips had to be extracted from the fuel assemblies and from the whole primary circuit. But the opinions and motivations were diverse (and sometimes contradictory); amongst them :

- the reason why only new assemblies were affected could be that only a thin protective layer of zirconium oxide is present (a beneficial aspect of Zircaloy corrosion!)
- the erosion of the cladding by chips can spread leakage and threaten the whole core
- flow blockage by chips can create local burnout or boiling with induced Zry corrosion (even more severe at shutdown conditions, i.e. no or low flow)
- chips may block a control rod ("CR") and prevent it from dropping in a safety related event
- carbon steel chips can induce corrosion of SS parts, i.e. assembly bottom end pieces.

4.1.4. The inspection and clean-up involved the whole primary circuit :

- upper reactor internals : bottom plate interior of CR guide tubes, CR drive mechanisms in the stand-pipes of the vessel head. Some chips were found.



- lower reactor internals, reactor vessel bottom, core barrel and core support plates. No or few chips were found there.
- reactor vessel nozzles and the hot and cold legs (the latter, from vessel to pumps and from SG to pump); this was performed by a small submarine equipped with a camera. The hot leg internal surfaces looked black and dirty and the cold leg ones brighter. No chips.
- SG's
- pressurizer. No chips.

The amount of chips collected by that time was sufficient to analyse the two categories and to confirm their source :

- small hard SS chips, resulting from the drilling through the SS cladding of the SG nozzle
- larger soft and rusty carbon steel chips, resulting from the drilling into the nozzle wall.

4.1.5. The fuel element clean-up was being performed in parallel in the spent fuel pool and consisted in the following successive steps :

- extraction of the externally visible chips, by a little tool ("piddler") fitted on a camera, since this equipment was available and the personnel trained. It allowed to see only the peripheral rods of the assembly.
- high velocity water flow cleaning, in a specially built equipment (the "washing machine") allowing to alternate normal and counter current flow, while collecting the chips in a cyclone
- control on an inspection stand
- leak testing by an elaborate ultra-sonic equipment; this detected 4 more leakers, increasing the total to 7 (out of the 121 assemblies constituting the core)
- water jet cleaning of the interior of the CR guide thimble.

4.1.6. The total amount of recuperated chips is indicated in Table 10. It is in majority large C steel chips, for which the fuel assemblies acted as an efficient filter.

4.1.7. After reloading the core with 80 assemblies present in the previous cycle and 41 older spent assemblies, the unit was back on the grid 155

days after its stop. For a large (1000 MWe) power plant, this loss of availability would represent 100 to 130 M\$. To it must be added 2 M\$ registered as direct expenses (services, machines, core calculations, etc.) and 1 M\$ estimated for indirect costs and the transport and repair of defective fuel assemblies. This is the present situation : additional fuel leakage, as a consequence of previous damage, and the unavoidable SG leakage might again lead to the technical specification limit being reached, with the obligation to shutdown for further fuel replacement.

#### 4.2. CNA chip occurrences

In 1978, debris alike the KCD 2 carbon steel chips (in envelope size but not in shape) were carried around the primary circuit, as a result of the failure of a metallic seal ring. These debris were also observed to be caught between the fuel rods near the grids. Safety and performance analyses [15] indicated that the presence of these debris was unlikely to present a threat preventing further utilization of these assemblies. The debris were therefore left in place and the assemblies were reloaded and irradiated to standard discharge burnup. No occurrence of fuel failure was noticed.

#### 4.3. Tihange 1 baffle jetting

The core consists of 151 assemblies, approximately one third of which are fresh. Tihange 1 is one of the PWR's affected by baffle jetting; most of the remedies failed to cure the defect, which has rather the tendency to extend over the years. This defects led to the failure of fresh fuel assemblies located in front of the baffle leaks; the number of failed assemblies discovered during the annual refuelling shutdowns from 1980 to february 1983 were successively 2, 6, 8 and 7. Some of these assemblies were successfully repaired [16]. The design of the subsequent assemblies to be located at baffle jet affected locations was modified, by replacing two fuel rods by dummy rods and adding local shroud pieces, to make them baffle jet resistant.

#### 4.4. Lessons learned

"Mechanical" coolant/cladding interaction has been the main cause of fuel failure in Belgian power plants during the last years. It showed the frustrating tendency to affect only fresh fuel (i.e. fuel during its first irradiation cycle).

With the SG leakage rate experienced in some PWR's, secondary circuit activity has become the main limiting factor for the amount of leaking fuel admissible in the core. Results of previous surveys on the economic impact of fuel failure [e.g. 17] should be revised in this perspective.

In some instances (e.g. baffle jetting), proper fuel assembly design can attenuate the propensity of the fuel to fail. In other cases (e.g. circulating debris), the cladding properties seem to play a significant role; the mechanism of clad failure when a debris is caught in a fuel assembly should be clarified (burnout, corrosion and/or erosion?).

Coolant specifications and control techniques (including sampling) regarding "suspended solids" should be revised. This includes an assessment of the capability of loose-part monitoring systems.

#### 5. CONCLUSIONS

Coolant/Cladding Interaction ("CCI") has been the major cause of fuel failure in the Belgian plants over the recent years. With only 7 nuclear power plants in operation, this observation might not be representative of the world-wide situation. It suggests however that adequate attention should be devoted to CCI. As was done in the past for PCI (pellet/cladding interaction), it should include a proper understanding of the parameters affecting the phenomena and a search for remedies.

Water chemistry has been investigated since many years and interesting data bases already exist, mainly on separate effects. An operating power plant is however a complex environment with frequent disturbances to steady

state conditions. A comprehensive understanding of the interactive parameters is likely to reduce the inconveniences the plant operator has to cope with and even to afford him additional flexibility. For instance, crud deposits on the cladding should be minimum under operating conditions, but are probably not important in shutdown conditions; in fact, coolant impurities are best disposed off as crud on spent fuel to be reprocessed than as soluble ions caught in IX purification resins to be conditioned at the power plant site.

"Suspended solids" is a part of the primary coolant specification which deserves adequate attention and backfitting, as experience develops.

Finally, as some CCI events are a consequence of interactive chemical, heat transfer and mechanical effects, experts should not limit their considerations one single of those aspects only.

#### 6. ACKNOWLEDGEMENT

The data presented in this paper result from the work of research, engineering and operating teams of numerous organizations, amongst which BELGONUCLEAIRE, SCK/CEN and KCD. The authors are particularly grateful to Mr. K. Huys (KCD), who provided the update summarized in section 4.1.

#### REFERENCES

- [1] R. Vanbrabant, P. De Regge  
Study of the Corrosion Products in the Primary System of PWR plants as the Source of Radiation Fields Build-up, IAEA-SM-264/17, Vienna, Nov. 82 and BLG 552, Jan. 82.
- [2] EPRI NP-2681, Oct. 1982  
Evaluation of Co Sources in W-designed 3- and 4-loop Plants.
- [3] EPRI NP-2685, Oct. 1982  
Co Source Identification Program.
- [4] P. Cohen  
The chemistry of water and solutions at high temperatures for application to corrosion in power systems, WARD-5788, 1972.

- [5] A.O. Allen  
The radiation chemistry of water and aqueous solutions, Van Nostrand, Princeton, N.J. 1961.
- [6] D.D. MacDonald, T.E. Rimmery  
The thermodynamics of metal oxides in water-cooled nuclear reactors, AECL-4140.
- [7] T.E. Rimmery, D.D MacDonald  
The thermodynamics of selected transition metal ferrites in high temperature aqueous systems., BNES, 1977.
- [8] F. Garzarolli et al  
KNU Results on Waterside Corrosion of Zry in PWR's and BWR's. Presentation to this specialists' meeting.
- [9] H. Bairiot, M. Billiaux  
Influence of Crud and Corrosion on the Safety Analysis of PWR Fuel Rods. IWCFPT/11. - IAEA Specialists' Meeting, San Miniato, Oct. 1981.
- [10] A. Lhost, H. Bairiot  
Irradiation de combustibles mixtes  $UO_2$ - $PuO_2$  dans le réacteur BR3/PWR EUR 4004 f, 1969.
- [11] E. Trauwaert, B. van Outryve d'Ydewalle  
BELGONUCLEAIRE internal document, December 1975.
- [12] M. Lippens et al  
Fuel Rods Failure Induced by Waterside Corrosion in Reactor BR 3. IWCFPT/11 - IAEA Specialists' Meeting, San Miniato, Oct. 1981.
- [13] H. Bairiot  
High Burnup : Status and Expectations., IAEA-CN-42/49, International conference on Nuclear Power Experience, Vienna, September 1982.
- [14] H. Breemer et al  
Experience of high Burnup Assemblies in the Dodewaard BWR., IWCFPT/10, IAEA Specialists' Meeting, Mol, March 1981.
- [15] BELGONUCLEAIRE proprietary report
- [16] L.F. Van Swan et al  
Poolside Fuel Assembly Reconstruction. TANSAO 40 (1982), ENC-3, Brussel, April 1982.
- [17] D.G. Franklin  
Economic Incentives for improved Core Materials Performance, Trans ANS, vol 35, 1980.

Table 1

**COMPARATIVE CHARACTERISTICS OF THE BELGIAN POWER PLANTS**  
(The figures in parenthesis represent local peak conditions.)

Power plant		BR 3	CNA	DOEL 1 & 2	Tihange 1	DOEL 3 & Tihange 4	DOEL 4 & Tihange 3
Start of commercial operation		1962	1976	1974 & 75	1975	1982 & 83	1984
Thermal power	MWth	41	1000	1200	2700	2800	3000
Power density	kW/l	78 (174)	69 (159)	103 (235)	100 (204)	104 (226)	96 (216)
LHGR	W/cm	205 (530)	167 (420)	225 (510)	227 (510)	184 (410)	170 (400)
Heat flux	W/cm <sup>2</sup>	69 (170)	54 (120)	67 (150)	68 (150)	62 (140)	57 (130)
Coolant pressure	bar	140	140	156	156	156	156
Reactor inlet	C	255	266	287 (289)	284 (290)	287 (290)	293
Average coolant	C	261 (280)	283	302	303	307	311
Core outlet	C	270 (306)	306 (334)	319 (341)	322 (345)	326 (343)	330 (345)
Water saturation	C	335	336	344	345	345	345
Maximum clad OD*	C	298 (347)	320 (349)	339 (356)	342 (355)	338 (354)	340 (350)

\* i.e. at the external surface of the oxide layer or crud deposit, if present.

Table 2

**CHARACTERISTICS OF DODEWAARD AS COMPARED TO MODERN BWR'S**

Power plant		Dodewaard	large BWR
Start commercial operation		1969	1978-1984
Thermal power	MWth	163	2400-3300
Power density	kW/l	36 (112)	51 (110)
LHGR	W/cm	160 (490)	187 (380)
Heat flux	W/cm <sup>2</sup>	36 (110)	48 (94)
Coolant pressure	kg/cm <sup>2</sup>	71	71
Reactor inlet	C	200	205
Reactor outlet	C	286	286

**Table 3**

**PRIMARY COOLANT WATER PROPERTIES FOR KCD 1 + 11 (\*\*)**

Data	KCD 1		KCD 11	
pH	6.7 ± 0.3		6.5 ± 1.1	
H <sub>2</sub>	35.4 ± 4.7		35.7 ± 5.7	cm <sup>3</sup> /kg H <sub>2</sub> O
Cl <sup>-</sup>	13.8 ± 4.6		18.6 ± 8.2	µg/l
SiO <sub>2</sub>	185.7 ± 83.9		162.8 ± 65.2	µg/l
F <sup>-</sup>	1.7 ± 0.8		6.5 ± 5.3	µg/l
O <sub>2</sub>	2.2 ± 1.2		2.2 ± 0.6	µg/l
Na <sup>+</sup>	< 10		< 10	µg/l
<sup>7</sup> Li <sup>+</sup> (*)	1447.4 ± 529.9		1453.3 ± 428.1	µg/l
K <sup>+</sup>	< 20		< 20	µg/l
Conductivity	15.5 ± 5.0		17.4 ± 4.7	µS/cm
B (*)			see figure 1	ppm

(\*) function of burnup

(\*\*) measurement during the reactor cycles

**Table 4**

**CONCENTRATION OF CORROSION PRODUCTS IN THE PRIMARY COOLANT OF KCD 1 (µg/l)**

Ni		5.4 ± 4.1
Mg		10.1 ± 1.9
Fe		19.5 ± 17.1
Si		62.2 ± 138.5
Al		3.9 ± 2.8
Cr		1
Mn		3
Ba, Cd, Be, Co, Cu		1
Sn, Mo		5
Pb		10
As, Sb		100

**Table 5**

**AMOUNT OF CRUD FILTERABLE OUT OF THE COOLANT (KCD 1)**

Filtermembrane with pore diameter (µm)	2		1		0.4		0.2		0.1
Crud (mg/l)	0.14		0.12		0.17		0.06		0.008

Table 6

## RADIOACTIVITY IN THE PRIMARY COOLANT (\*)

Isotope	KCD 1	KCD 2	Unit
Total $\gamma$	(1.11 $\pm$ 0.11) E7	(1.11 $\pm$ 0.04) E7	s <sup>-1</sup> l <sup>-1</sup>
Total $\beta$	(3.70 $\pm$ 7.40) E6	(4.44 $\pm$ 4.07) E6	s <sup>-1</sup> l <sup>-1</sup>
<sup>3</sup> H	1.04 E10	9.25 E9	Bq m <sup>-3</sup>
<sup>135</sup> Xe	2.92 E6		Bq m <sup>-3</sup>
<sup>51</sup> Cr	2.41 E6	5.55 E7	Bq m <sup>-3</sup>
<sup>131</sup> I	5.18 E5		Bq m <sup>-3</sup>
<sup>187</sup> M	1.33 E7		Bq m <sup>-3</sup>
<sup>133</sup> I	7.40 E6		Bq m <sup>-3</sup>
<sup>58</sup> Co	2.52 E7	4.07 E7	Bq m <sup>-3</sup>
<sup>134</sup> Cs		3.59 E6	Bq m <sup>-3</sup>
<sup>137</sup> Cs		4.81 E6	Bq m <sup>-3</sup>
<sup>54</sup> Mn		2.52 E6	Bq m <sup>-3</sup>
<sup>60</sup> Co		1.92 E6	Bq m <sup>-3</sup>

(\*) : 1.04 E 10 = 1.04 10<sup>10</sup>

Table 7

## SPECIFIC ACTIVITY OF CRUD (KCD 1) (Bq/mg)

Isotope	Distribution of crud according to particle size ( $\mu$ m)				
	$\geq 2$	1 - 2	0.4 - 1	0.2 - 0.4	0.1 - 0.2
<sup>58</sup> Co	4.43 E4	4.40 E3	4.00 E3	4.00 E3	1.76 E4
<sup>60</sup> Co	4.81 E2	1.11 E2	7.40 E1	7.40 E1	1.48 E2
<sup>59</sup> Fe	1.48 E2		7.40 E1	7.40 E1	
<sup>51</sup> Cr	4.18 E3	5.18 E2	4.81 E2		
<sup>54</sup> Mn	3.70 E2	1.48 E2	2.96 E2	4.07 E2	5.18 E2
$\Sigma$	4.95 E4	5.18 E3	4.92 E3	4.55 E3	1.79 E4

Table 8

## CHEMICAL STRUCTURE OF CORROSION PARTICLES

Specimen	Main component	Minor component
Particles $\geq 0.45 \mu$ m KCD 2 (Sample 1)	$\alpha$ Fe and/or Cr	Fe <sub>3</sub> O <sub>4</sub> a/o (Fe,Mg)(Cr,Fe) <sub>2</sub> O <sub>4</sub>
Particles $\geq 0.45 \mu$ m KCD 2 (Sample 2)	Fe <sub>3</sub> O <sub>4</sub> a/o (Fe,Mg)(Cr,Fe) <sub>2</sub> O <sub>4</sub>	
Crud deposits on reactor vessel KCD 2	Fe <sub>3</sub> O <sub>4</sub> a/o (Fe,Mg)(Cr,Fe) <sub>2</sub> O <sub>4</sub>	

Table 9

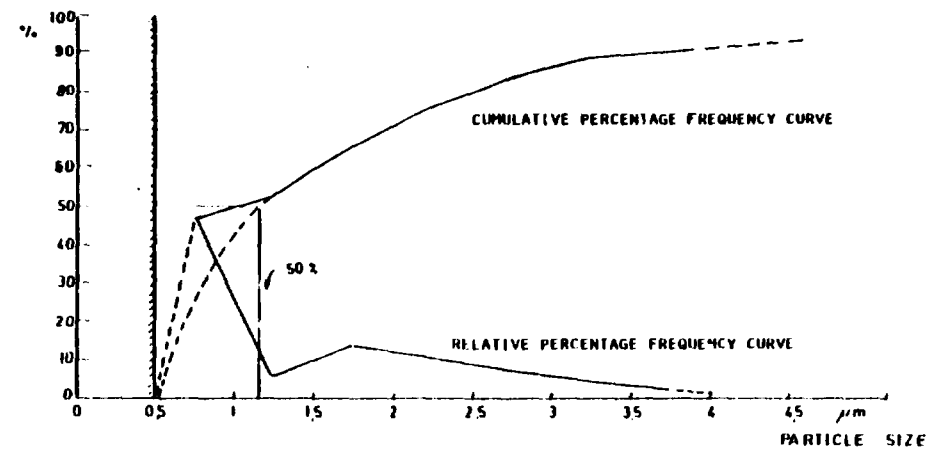
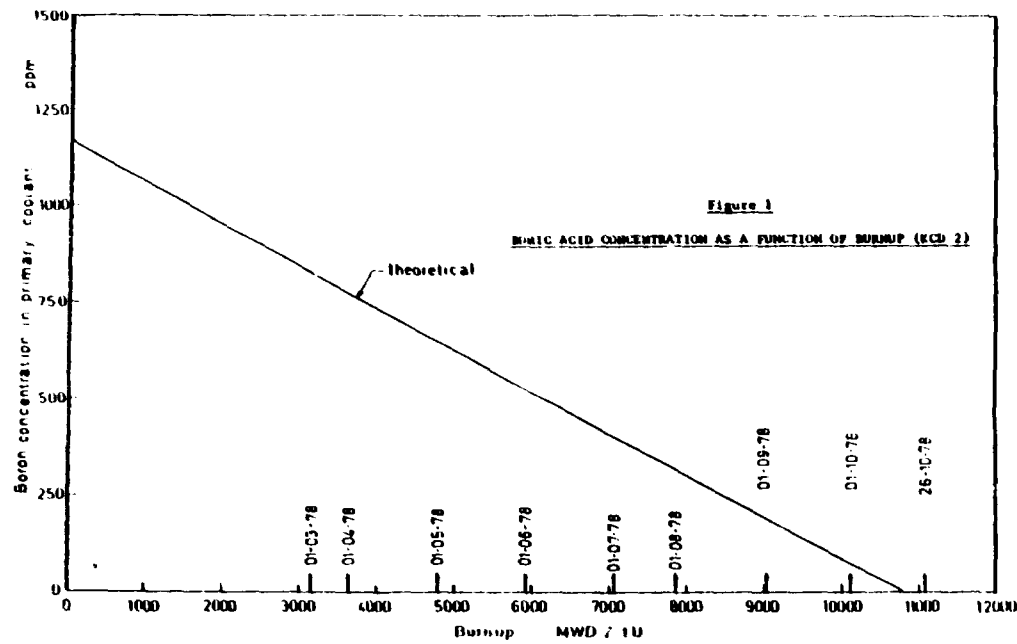
PARTICLES IN SUSPENSION AS A FUNCTION OF TIME ( $\mu$ g/l)

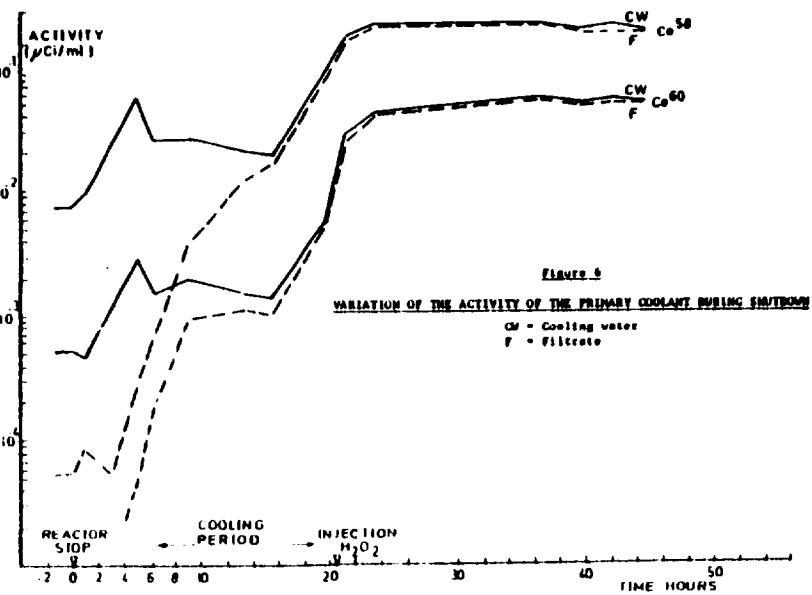
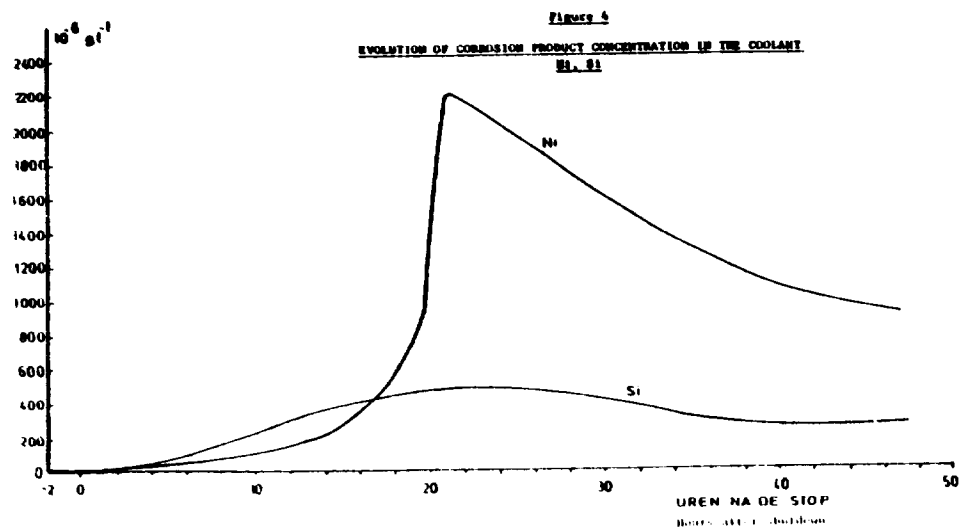
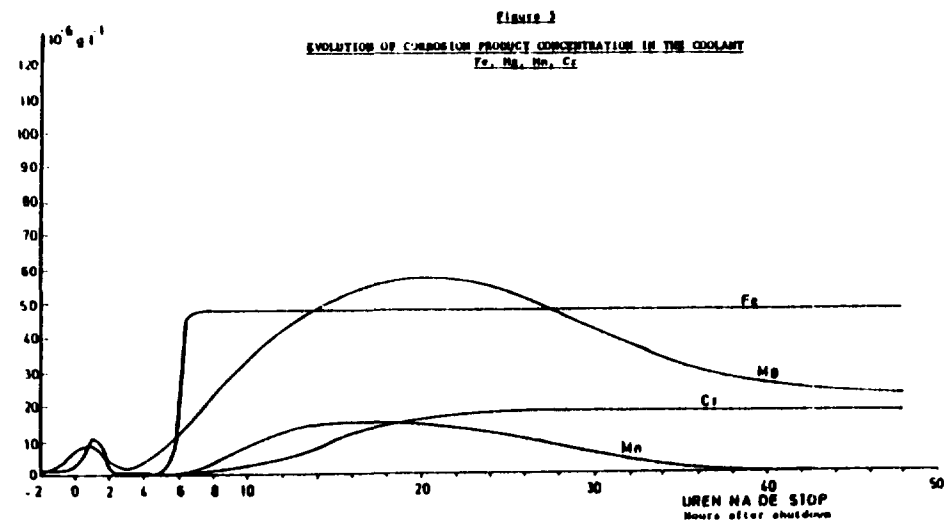
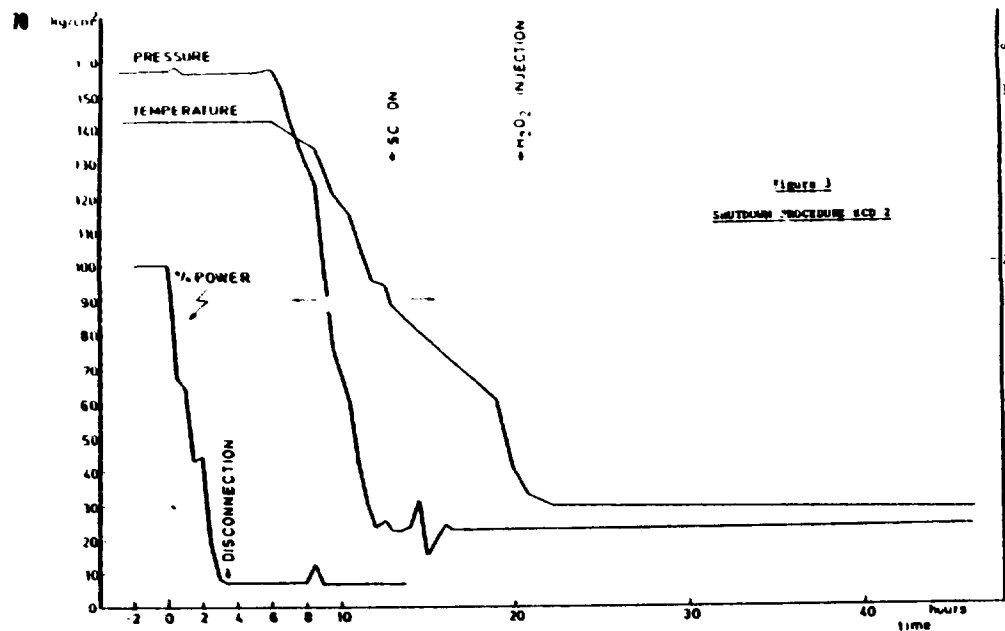
Element	Time after shutdown			
	- 2	+ 6.5	+ 13	+ 45.5
Mn	< 1	< 1	< 1	< 1
Fe	< 2	3	< 2	3
Cr	< 1	2	< 1	< 1
Si	< 2	< 2	< 2	< 2
Al	< 5	< 5	< 5	< 5
Ca	< 1	< 1	< 1	< 1
Ni	3	10	< 1	9
Ti	< 1	< 1	< 1	< 1
Mg	< 1	< 1	< 1	< 1

Table 10

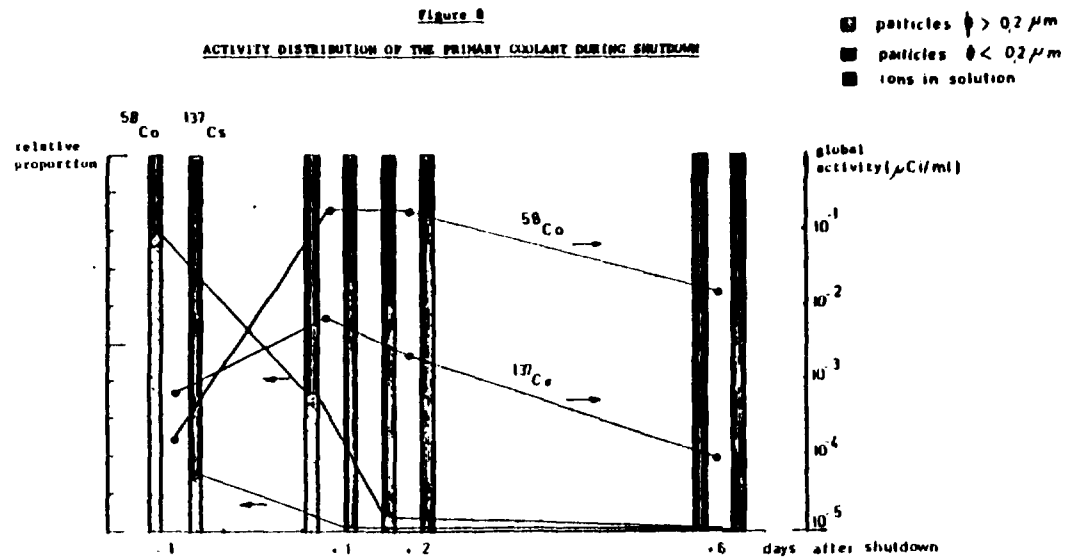
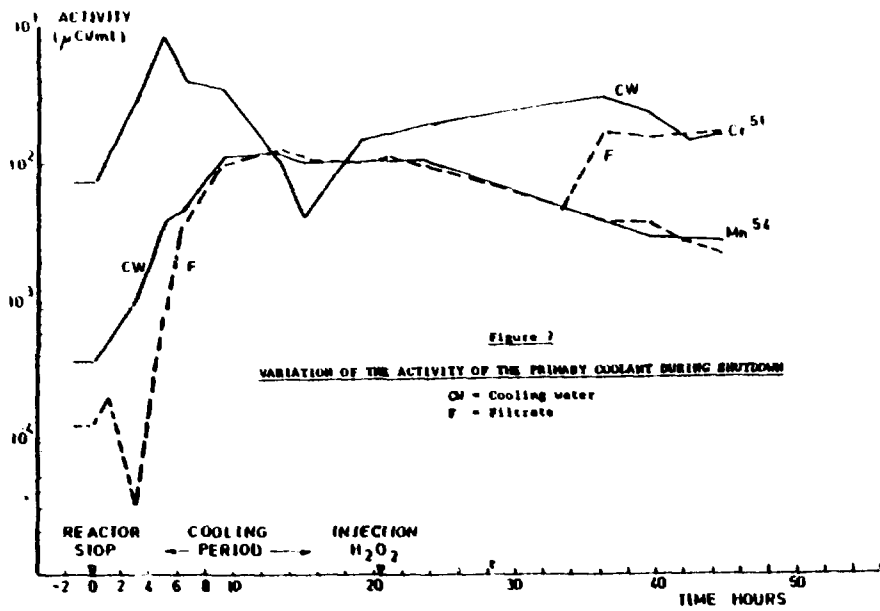
KCD 2 CHIP INCIDENT - RECUPERATED MATERIAL

Clean-up Operation	Quantity (g)	Proportion (%)	
		SS	C at
Primary circuit	73	59	41
Reactor pool	36	68	29
"Piddling"	220	5	95
"Washing"	16	65	35
Guide thimbles	0	nd	nd
Spent fuel pool	2	nd	nd
Fuel assembly subtotal	273	16	84
Total	348	25	75









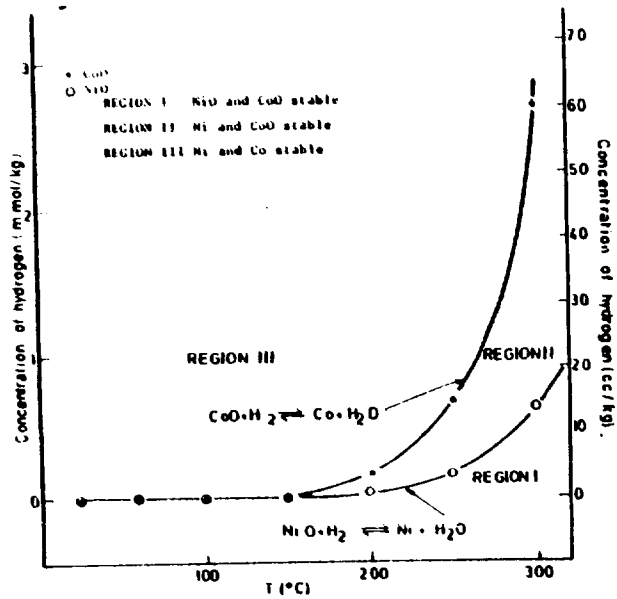


Figure 9  
EQUILIBRIUM CONCENTRATION OF HYDROGEN IN H<sub>2</sub>O AS A FUNCTION  
OF TEMPERATURE FOR THE REACTIONS

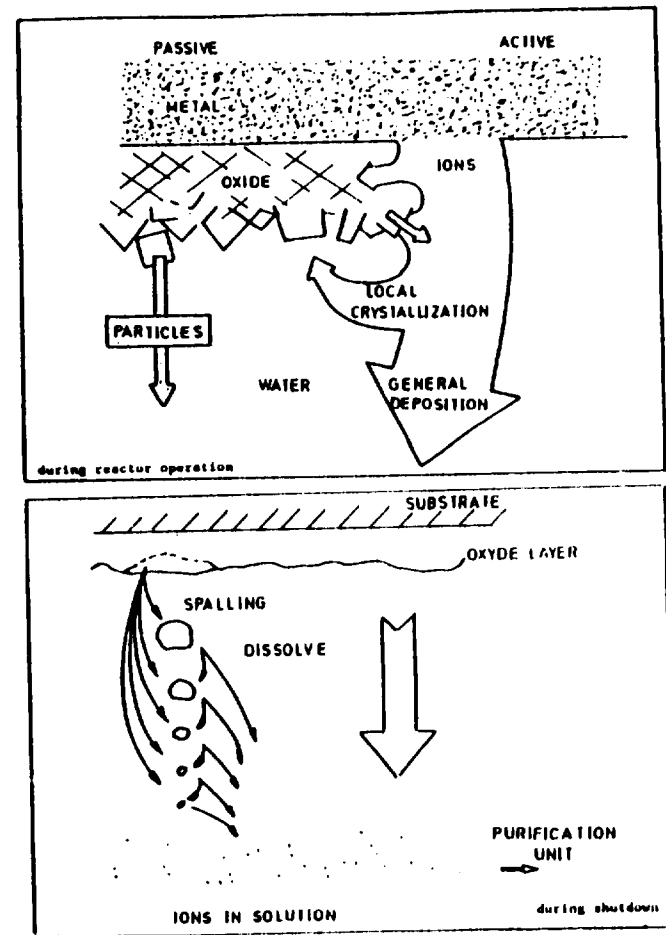
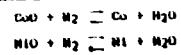


Figure 10  
CORROSION OF STRUCTURAL MATERIALS AS DRIVING FORCE FOR TRANSPORT OF PARTICLES